

# Single-valued representation of unpolarized and polarized semi-inclusive deep inelastic scattering at next-to-next-to-leading order

Juliane Haug\* and Fabian Wunder†  
*Institute for Theoretical Physics, University of Tübingen*  
*Auf der Morgenstelle 14, 72076 Tübingen, Germany*  
 (Dated: May 23, 2025)

We revisit the recently published analytic results for unpolarized and polarized semi-inclusive deep inelastic scattering (SIDIS) at next-to-next-to-leading order (NNLO) in QCD. These expressions for the hard scattering coefficients contain case distinctions in the kinematic  $(x, z)$  plane splitting the analytic result in four regions. By re-expressing the coefficient functions in terms of single-valued polylogarithms we remove these case distinctions and can present a unified result valid in the entire kinematic range of SIDIS. This reduces the length of the overall expressions by 30% to 60%.

Keywords: perturbative QCD, semi-inclusive DIS, single-valued polylogarithms

## INTRODUCTION

Semi-inclusive deep inelastic scattering (SIDIS) is one of the cornerstones of the physics program at the upcoming Electron Ion Collider (EIC) [1, 2]. By probing hadrons created in the high-energy scattering of (polarized) electrons off (polarized) protons SIDIS allows for accessing (polarized) parton distributions (PDFs) and fragmentation functions (FFs) [3]. In the context of PDF and FF determination SIDIS is of particular importance to achieve flavor separation. At present, SIDIS data exists from several experiments [4–8].

The theoretical description of SIDIS is based on the factorization of the process into long-distance non-perturbative hadron dynamics captured by PDFs and FFs and short-distance hard scattering coefficient functions which are accessible by perturbative quantum chromo dynamics (pQCD). To achieve high precision in the PDF and FF extraction, relevant also for new physics searches especially in the context of the EIC [9], a highly accurate calculation of the perturbative part is paramount. Hence it has been an important achievement that SIDIS coefficient functions have recently become available to full NNLO for both the unpolarized and polarized case [10–14]. This allows for the inclusion of SIDIS data in future fully NNLO fits of polarized parton distributions. So far only approximate NNLO based on threshold resummation [15, 16] could be used necessitating cuts on the data to be included in the MAPPDF-pol1.0 [17] and BDSSV24 [18] fits while NNPDFpol2.0 [19] did not include SIDIS data.

In this letter we revisit the analytic NNLO results for SIDIS. These contain case distinctions in the kinematic  $(x, z)$  plane splitting the result into four regions. By re-expressing the coefficient functions in terms of a particular version of single-valued polylogarithms (SVPs) we remove these case distinctions and present a result valid in the entire kinematic range of SIDIS. As depicted in figure 1, this substantially reduces the length of the overall coefficient functions by 30% to 60%, nearly reducing it to the length of the part of the original ex-

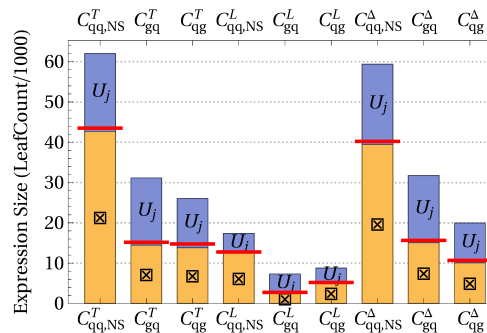


Figure 1. Comparison of expression sizes before (full bars) and after (horizontal red lines) removing case distinctions.  $U_j$  indicates all parts of the expressions from [11, 12] involving case distinctions,  $\boxtimes$  the rest (see eq. (9)). Expressions are consistently sorted, **LeafCount** (number of indivisible subexpressions in **Mathematica**) serves as proxy to measure expression length.

pressions which does not involve case distinctions. The benefit of this is twofold. Phenomenologically, in the context of PDF fits it is of interest to have compact expressions that can be calculated quickly since they need to be evaluated millions of times. Closely related, due to the absence of case distinctions, our results may help establishing an analytic Mellin transform of the cross section, highly desirable for PDF extraction. More formally, it is intriguing to see SVPs appearing for the first time in the simplification of observable level quantities in QCD beyond the Regge limit [20], an idea that might generalize to other processes and higher-loop calculations. So far SVPs have seen use on amplitudes [21–25] and conformal theories [26].

The remainder of this letter is structured as follows. First we recall the fundamentals of the SIDIS process and introduce essential notation. Readers familiar with [11, 12] might skip directly to the third section where the case distinctions present in the NNLO coefficient functions are discussed. We proceed by removing these through introducing SVPs before we conclude. The results and a numerical implementation of SVPs are provided as **Mathematica** readable ancillary files.

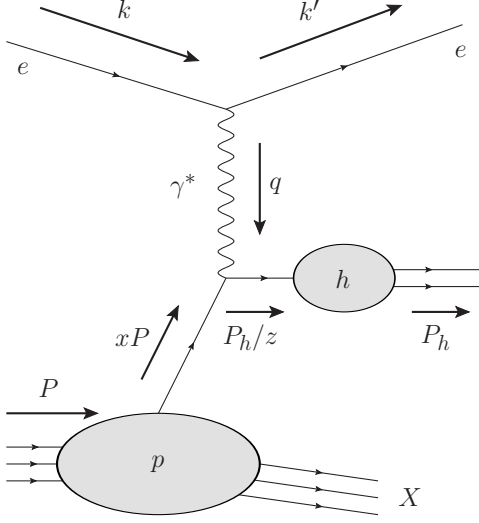


Figure 2. Sketch of the SIDIS process  $e(k)p(P) \rightarrow e(k')h(P_h) + X$  in the parton model. Here  $e$  denotes the scattered electron,  $\gamma^*$  the intermediate virtual photon,  $p$  the incoming proton,  $h$  the identified hadron, and  $X$  the proton remnant (including all unidentified particles in the final state). In SIDIS the electron momentum and the identified hadron's longitudinal momentum are measured. Radiative corrections are not included in the picture.

### SIDIS KINEMATICS, FACTORIZATION, AND COEFFICIENT FUNCTIONS

The kinematics of the process  $e(k)p(P) \rightarrow e(k')h(P_h) + X$  is determined by the invariant mass of the intermediate photon  $Q^2 = -q^2$ , where  $q = k - k'$  is fixed by the observed electron, the energy transfer of the electron to the proton  $y = (P \cdot q)/(P \cdot k)$  and the hadronic variables

$$x = \frac{Q^2}{2P \cdot q}, \quad z = \frac{P \cdot P_h}{P \cdot q}. \quad (1)$$

The Bjorken variable  $x$ , familiar from inclusive DIS, characterizes the longitudinal momentum fraction of the parton within the incoming proton, while the fragmentation variable  $z$  describes the longitudinal momentum fraction of the outgoing parton carried by the identified hadron. Note that SIDIS as discussed here is inclusive in the observed hadron's transverse momentum. The triple differential cross section for the unpolarized case reads

$$\frac{d^3\sigma^h}{dx dy dz} = \frac{4\pi\alpha^2}{Q^2} \left[ \frac{1 + (1-y)^2}{2y} \mathcal{F}_T^h(x, y, Q^2) + \frac{1-y}{y} \mathcal{F}_L^h(x, y, Q^2) \right], \quad (2)$$

where  $\alpha$  is the electromagnetic fine-structure constant and  $\mathcal{F}_{T/L}^h$  are transverse respectively longitudinal structure functions. The structure functions can be collinearly factorized up to higher-twist corrections in

the form

$$\mathcal{F}_{T/L}^h(x, z, Q^2) = \sum_{a,b} \int_x^1 \frac{d\hat{x}}{\hat{x}} \int_z^1 \frac{d\hat{z}}{\hat{z}} f_{a/p}\left(\frac{x}{\hat{x}}, \mu_F^2\right) \times D_{h/b}\left(\frac{z}{\hat{z}}, \mu_A^2\right) \mathcal{C}_{ba}^{T/L}(\hat{x}, \hat{z}, \mu_R^2, \mu_F^2, \mu_A^2), \quad (3)$$

where the sum runs over all partons  $a, b = q, \bar{q}, g$ .  $f_{a/p}$  denotes the PDF to find parton  $a$  in the proton,  $D_{h/b}$  denotes the FF for the fragmentation of parton  $b$  into hadron  $h$ ;  $\mu_R^2$ ,  $\mu_F^2$ , and  $\mu_A^2$  are the renormalization, factorization, and fragmentation scales respectively.

For longitudinally polarized incoming electrons and protons producing an unpolarized hadron in the final state the analogous differential cross section

$$\frac{d^3\Delta\sigma^h}{dx dy dz} = \frac{4\pi\alpha^2}{Q^2} (2-y) g_1(x, z, Q^2) \quad (4)$$

is parameterized by only one polarized structure function  $g_1$ . The factorization analogous to eq. (3) in the polarized case reads

$$2g_1(x, z, Q^2) = \sum_{a,b} \int_x^1 \frac{d\hat{x}}{\hat{x}} \int_z^1 \frac{d\hat{z}}{\hat{z}} \Delta f_{a/p}\left(\frac{x}{\hat{x}}, \mu_F^2\right) \times D_{h/b}\left(\frac{z}{\hat{z}}, \mu_A^2\right) \mathcal{C}_{ba}^\Delta(\hat{x}, \hat{z}, \mu_R^2, \mu_F^2, \mu_A^2), \quad (5)$$

where  $\Delta f_{a/p}$  denotes the polarized PDF. The partonic coefficient functions in both unpolarized and polarized cases only depend on the hard interaction with the virtual photon and can be calculated in perturbative QCD. Expanding up to NNLO in the strong coupling  $\alpha_s$  it is

$$\mathcal{C}_{ba}^i = \mathcal{C}_{ba}^{i,(0)} + \frac{\alpha_s(\mu_R^2)}{2\pi} \mathcal{C}_{ba}^{i,(1)} + \left( \frac{\alpha_s(\mu_R^2)}{2\pi} \right)^2 \mathcal{C}_{ba}^{i,(2)} + \mathcal{O}(\alpha_s^3), \quad (6)$$

where  $i = T, L, \Delta$ . The coefficients up to NLO have been known for some time [27, 28]. Following the notation of [11, 12, 29], the seven partonic channels at NNLO are

$$\begin{aligned} \mathcal{C}_{qq}^{i,(2)} &= \mathcal{C}_{\bar{q}\bar{q}}^{i,(2)} = e_q^2 \mathcal{C}_{qq}^{i,\text{NS}} + \left( \sum_j e_{q_j}^2 \right) \mathcal{C}_{qq}^{i,\text{PS}}, \\ \mathcal{C}_{\bar{q}q}^{i,(2)} &= \mathcal{C}_{q\bar{q}}^{i,(2)} = e_q^2 \mathcal{C}_{\bar{q}q}^i, \\ \mathcal{C}_{q'q}^{i,(2)} &= \mathcal{C}_{\bar{q}'\bar{q}}^{i,(2)} = e_q^2 \mathcal{C}_{q'q}^{i,1} + e_{q'}^2 \mathcal{C}_{q'q}^{i,2} + e_q e_{q'} \mathcal{C}_{q'q}^{i,3}, \\ \mathcal{C}_{\bar{q}'q}^{i,(2)} &= \mathcal{C}_{q'\bar{q}}^{i,(2)} = e_q^2 \mathcal{C}_{q'q}^{i,1} + e_{q'}^2 \mathcal{C}_{q'q}^{i,2} - e_q e_{q'} \mathcal{C}_{q'q}^{i,3}, \\ \mathcal{C}_{gq}^{i,(2)} &= \mathcal{C}_{g\bar{q}}^{i,(2)} = e_q^2 \mathcal{C}_{gq}^i, \\ \mathcal{C}_{qg}^{i,(2)} &= \mathcal{C}_{\bar{q}g}^{i,(2)} = e_q^2 \mathcal{C}_{qg}^i, \\ \mathcal{C}_{gg}^{i,(2)} &= \left( \sum_j e_{q_j}^2 \right) \mathcal{C}_{gg}^i, \end{aligned} \quad (7)$$

where  $q$  and  $q'$  denote (anti-)quarks of different flavor, NS is the non-singlet and PS the pure-singlet contribution.

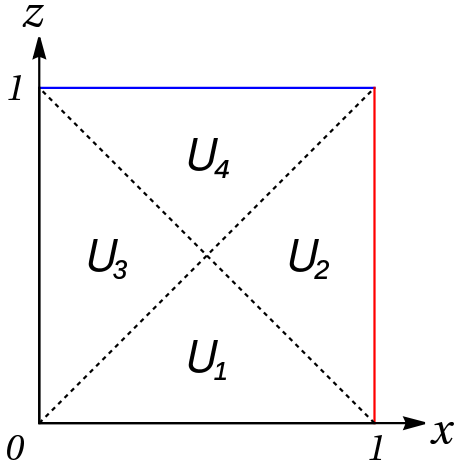


Figure 3. The four regions of SIDIS for which there are case distinctions in the NNLO coefficient functions as presented in [10–14]. The red and blue boundaries depict the kinematic endpoints for  $x$  respectively  $z$  where physical thresholds are present.

### CASE DISTINCTIONS IN NNLO SIDIS CROSS SECTION

The coefficients of eq. (7) have been recently calculated independently by two groups in [10–14]. The results of both are in (numerical) agreement and available as supplemental material to the aforementioned publications. For both the unpolarized and polarized structure functions, the expressions are of considerable length. Overall the results of [11, 12] are more compact in comparison to [14], most importantly in regards to a minimal number of polylogarithms. Hence we choose the former as baseline for our simplified results, however we explicitly checked that the presented method works analogously for the latter.

Notably, in the channels  $q \rightarrow q$  (NS),  $q \rightarrow g$ , and  $g \rightarrow q$ , the analytic representation requires case distinctions between four regions in the  $(x, z)$ -plane. These regions are depicted in figure 3 and follow the notation of [30] which was applied in [11, 12]. In the language of [31] they are given by

$$\begin{aligned} U_1 &= [x \geq z, x \leq 1 - z], & U_2 &= [x \geq z, x \geq 1 - z], \\ U_3 &= [x \leq z, x \leq 1 - z], & U_4 &= [x \leq z, x \geq 1 - z], \end{aligned} \quad (8)$$

furthermore the combined regions  $\boxtimes = \sum_{j=1}^4 U_j$ ,  $R_1 = U_1 + U_3$ ,  $R_2 = U_2 + U_4$ ,  $T_1 = U_3 + U_4$ , and  $T_2 = U_1 + U_2$  are used to present the coefficient functions. Hence the coefficient functions in [11, 12] have the generic form

$$\begin{aligned} C_{ba}^{i,(2)} &= C_{ba}^{i,(2),\boxtimes} + \sum_{j=1}^4 U_j C_{ba}^{i,(2),U_j} \\ &+ \sum_{j=1}^2 R_j C_{ba}^{i,(2),R_j} + \sum_{j=1}^2 T_j C_{ba}^{i,(2),T_j}, \end{aligned} \quad (9)$$

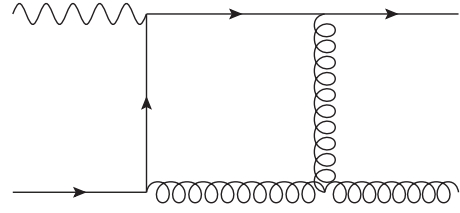


Figure 4. Illustrative one-loop box diagram contributing to the real-virtual correction at NNLO responsible for the spurious branch-cuts.

with different contributions  $C_{ba}^{i,(2),r}$  from the different regions  $r = \boxtimes, R_j, T_j, U_j$  to the overall coefficient function  $C_{ba}^{i,(2)}$ . The aim of this letter is to eliminate the distinction between regions and obtain a single-valued representation in the entire SIDIS range  $0 \leq x, z \leq 1$ . To achieve this we start from the origin of the case distinctions.

At NNLO there are three classes of QCD corrections, virtual-virtual, real-virtual, and real-real. The case distinction is only present in the channels that receive real-virtual corrections, i.e. those that are already present at NLO. The reason behind this is that the case distinctions originate solely from one-loop box diagrams like the one depicted in figure 4. The relevant analytical structure comes from the scalar box integral  $D_0$ , which in  $d = 4 - 2\varepsilon$  dimensions has the general form [32–39], valid not only for SIDIS kinematics but also Drell-Yan (DY) and single-inclusive annihilation (SIA),

$$\begin{aligned} D_0(s_1, s_2, q^2) &\sim \left(\frac{\mu^2}{-s_2}\right)^\varepsilon F_\varepsilon\left(\frac{-s_3}{s_1}\right) + \left(\frac{\mu^2}{-s_1}\right)^\varepsilon F_\varepsilon\left(\frac{-s_3}{s_2}\right) \\ &- \left(\frac{\mu^2}{-q^2}\right)^\varepsilon F_\varepsilon\left(\frac{-s_3 q^2}{s_1 s_2}\right), \end{aligned} \quad (10)$$

where  $F_\varepsilon(z) = {}_2F_1(1, -\varepsilon, 1 - \varepsilon; z)$  abbreviates a particular Gauss hypergeometric function, the  $s_i$  are Mandelstam variables,  $q^2$  is the invariant mass of the external off-shell particle, and  $\mu^2$  the renormalization scale. The prefactors  $(\dots)^\varepsilon$  in eq. (10) develop branch-cuts when the Mandelstam variables respectively  $q^2$  become positive. A change in sign of Mandelstam variables is associated with an interchange of incoming and outgoing particles, i.e. physically different kinematics shown in figure 5. Therefore those branch cuts are physical and the associated factors of  $i\pi$  may contribute in the absolute square of matrix elements as factors of  $\pi^2$ . However the hypergeometric functions  $F_\varepsilon$  in eq. (10) develop branch-cuts when their arguments become unity, for SIDIS these arguments are

$$\frac{1-x}{z}, \quad \frac{1-x}{1-z}, \quad \frac{(1-x)x}{(1-z)z}, \quad \frac{xz}{(1-x)(1-z)}, \quad \frac{(1-z)x}{(1-x)z}, \quad (11)$$

and also the respective inverses of the first three. They become unity at  $x = z$  or  $x = 1 - z$  giving rise to spu-

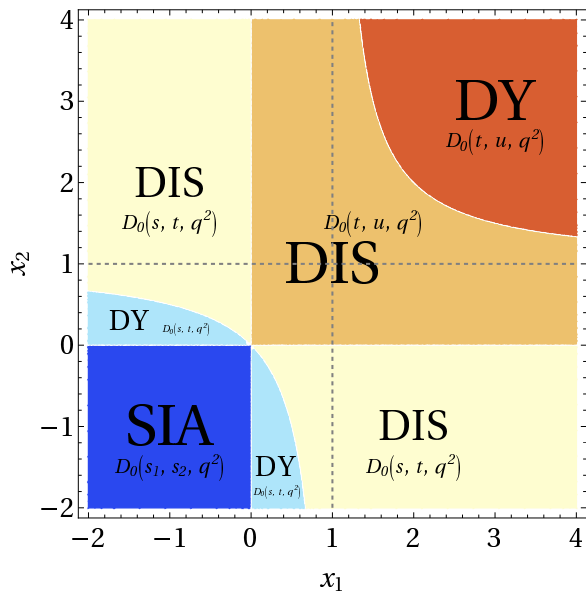


Figure 5. Branch cut structure of the one loop box integral. Each color coded region boundary corresponds to a physical branch-cut.  $x_{1,2}$  are ratios of Mandelstam variables defined in [38]. The dashed gray lines indicate the spurious branch cuts at  $x_i = 1$  induced by the hypergeometric functions in the representation of eq. (10) running right through the DIS regions.

rious branch-cuts within the SIDIS region that always cancel in the sum between the three  $F_\varepsilon$  in eq. (10). In [11, 12] and [10, 13, 14] those were treated in a similar way by transforming the arguments of the hypergeometric functions away from the region where the arguments become larger than 1 using hypergeometric transformations. This necessitates case distinctions based on the regions of figure 3 that remain in the final analytic result. The exact procedure employed by the different groups is detailed in section 5 of [30] respectively section C of [14].

In [38, 39] we have discussed how to treat the spurious branch-cuts in eq. (10) without introducing case distinctions by using a particular version of SVPs. In the next section we will recall this approach and apply it to the NNLO SIDIS coefficient functions.

### EXPRESSING SIDIS COEFFICIENT FUNCTIONS WITH SINGLE-VALUED POLYLOGARITHMS

Carefully tracking the branch-cut structure of the box-integral, we showed in [38] that the cancellation of spurious branch-cuts in eq. (10) can be achieved by replacing  $F_\varepsilon(x) \rightarrow |x|^\varepsilon \mathfrak{F}_\varepsilon(x)$ , where  $\mathfrak{F}_\varepsilon(x)$  is a single-valued version of the hypergeometric function. In par-

ticular it is real valued also for  $x > 1$  and given by

$$\mathfrak{F}_\varepsilon(x) = 1 - \ln \left| \frac{x}{x-1} \right| \sum_{n=1}^{\infty} \frac{\varepsilon^n}{n!} \ln^{n-1} \left| \frac{1}{x} \right| - \sum_{n=2}^{\infty} \varepsilon^n \mathcal{L}_n(x), \quad (12)$$

where  $\mathcal{L}_n(x)$  is a specific version of SVP [38, 40]

$$\mathcal{L}_n(x) = \sum_{k=0}^{n-1} \frac{\ln^k \left| \frac{1}{x} \right|}{k!} \text{Li}_{n-k}(x) + \frac{\ln^{n-1} \left| \frac{1}{x} \right|}{n!} \ln |1-x|. \quad (13)$$

SVPs have a rich pedigree in pure mathematics and mathematical physics [40–50] and have become a field of active research in the context of not only amplitude calculations [21–25, 51–54] but also the BFKL equation [20], soft-anomalous dimensions [55], thermal one-point functions [56], and energy correlators [26]. In the particular situation at hand, the appearance of single-valued functions is not coincidental but a consequence of the cancellation of spurious branch cuts build into the physical box integral.

Besides being single-valued and continuous on  $\mathbb{R}$  by construction, the SVPs of eq. (13) have the remarkable property of satisfying clean versions of polylogarithmic functional equations, i.e. free of product terms. Specifically, the inversion relation takes the form

$$\mathcal{L}_n(x) + (-1)^n \mathcal{L}_n\left(\frac{1}{x}\right) = \mathcal{L}_n(\text{sgn}(x) \infty), \quad (14)$$

with constants  $\mathcal{L}_{2n+1}(\pm\infty) = 0$ ,  $\mathcal{L}_{2n}(\infty) = 2\zeta_{2n}$  respectively  $\mathcal{L}_{2n}(-\infty) = 2(2^{1-2n} - 1)\zeta_{2n}$ . Moreover, these SVPs are bounded on  $\mathbb{R}$  which is welcome for numerical evaluation as well as the study of kinematic limits. More details on the SVPs of eq. (13) can be found in [38]. While we are led to single-valued versions of classical polylogarithms in this particular case because they appear in the  $\varepsilon$ -expansion of the one-loop box, demanding cancellation of spurious branch cuts for multi-loop generalizations should naturally lead to single-valued versions of generalized polylogarithms [48, 53].

In the NNLO SIDIS coefficient functions only polylogarithms of weight 2 appear together with region distinctions. Hence we only need to express the dilogarithm by its single-valued counterpart ,

$$\text{Li}_2(x) \rightarrow \mathcal{L}_2(x) - \ln |x| \ln(1-x) + \frac{\ln |x|}{2} \ln |1-x|, \quad (15)$$

in all regions and introduce absolute values for all logarithms developing branch-cuts outside their original region. Using the inversion relation eq. (14) on certain SVPs, the expression in all regions can be mapped onto a universal form allowing us to write the coefficient functions without case distinctions. Since the former four regions are now expressed by a single term, the size



of the part involving case distinctions shrinks by approximately 75%, as one would expect for an expression of similar complexity as the individual contributions to the four regions  $U_i$ . Finally sorting this contribution into the structure of the remaining part of the coefficient without case distinctions  $C_{ba}^{i,(2),\boxtimes}$  shrinks the overall coefficient function  $C_{ba}^{i,(2)}$  nearly to the size of  $C_{ba}^{i,(2),\boxtimes}$  (compare the horizontal red lines to the yellow bars in figure 1) resulting in overall size reductions ranging from 30% to 60%. To consistently and meaningfully compare the sizes of expressions, all coefficients have been sorted in a way closely matching [11, 12] with slight adaptations to accommodate for importing the expressions from FORM to Mathematica.

## CONCLUSION

In this letter we presented a significant compactification of the existing NNLO results for SIDIS. Leveraging the understanding how the underlying branch-cut structure of the loop integrals introduced spurious case distinctions in the results, we re-expressed the affected parts of the coefficient functions in terms of SVPs, the first use of the latter for observable level quantities in QCD beyond the Regge limit. This provides a representation both phenomenologically relevant in the context of (polarized) PDF extraction and theoretically interesting with a view to generalizing the applied method to branch-cuts in multi-loop multi-variable observables. All coefficient functions up to NNLO are given in Mathematica readable ancillary text files together with a numerical implementation of SVPs in part based on [57].

**Acknowledgments.**—We are grateful to Thomas Gehrmann and Sven Moch for stimulating discussions on the NNLO coefficient functions, to Ignacio Borsa for sharing insights into PDF fitting and helping to test the numerical implementation of SVPs, and to Werner Vogelsang for helpful comments on the manuscript. Special thanks go to Markus Löchner for initiating us into the secrets of rln2 in the supplemental material to [12]. We thank Renee Fatemi, Huey-Wen Lin and Werner Vogelsang for organizing the CFNS-INT Joint Program *Precision QCD with the Electron Ion Collider* and the Institute for Nuclear Theory at the University of Washington for its hospitality and the Department of Energy for partial support during the completion of this work. Figures 2 and 4 drawn with JaxoDraw [58]. This work was supported by Deutsche Forschungsgemeinschaft (DFG) through the Research Unit FOR 2926 (project 409651613).

---

\* juliane-clara-celine.haug@uni-tuebingen.de

† fabian.wunder@uni-tuebingen.de

- [1] A. Accardi *et al.*, Eur. Phys. J. A **52**, 268 (2016), arXiv:1212.1701 [nucl-ex].
- [2] R. Abdul Khalek *et al.*, Nucl. Phys. A **1026**, 122447 (2022), arXiv:2103.05419 [physics.ins-det].
- [3] E. C. Aschenauer, I. Borsa, R. Sassot, and C. Van Hulse, Phys. Rev. D **99**, 094004 (2019), arXiv:1902.10663 [hep-ph].
- [4] J. Ashman *et al.* (European Muon Collaboration), Z. Phys. C **52**, 361 (1991).
- [5] M. Derrick *et al.* (ZEUS), Z. Phys. C **70**, 1 (1996), arXiv:hep-ex/9511010.
- [6] C. Adloff *et al.* (H1), Nucl. Phys. B **485**, 3 (1997), arXiv:hep-ex/9610006.
- [7] A. Airapetian *et al.* (HERMES), Phys. Rev. D **87**, 074029 (2013), arXiv:1212.5407 [hep-ex].
- [8] C. Adolph *et al.* (COMPASS), Phys. Lett. B **764**, 1 (2017), arXiv:1604.02695 [hep-ex].
- [9] E. Hammou and M. Ubiali, (2024), arXiv:2410.00963 [hep-ph].
- [10] S. Goyal, S.-O. Moch, V. Pathak, N. Rana, and V. Ravindran, Phys. Rev. Lett. **132**, 251902 (2024), arXiv:2312.17711 [hep-ph].
- [11] L. Bonino, T. Gehrmann, and G. Stagnitto, Phys. Rev. Lett. **132**, 251901 (2024), arXiv:2401.16281 [hep-ph].
- [12] L. Bonino, T. Gehrmann, M. Löchner, K. Schönwald, and G. Stagnitto, Phys. Rev. Lett. **133**, 211904 (2024), arXiv:2404.08597 [hep-ph].
- [13] S. Goyal, R. N. Lee, S.-O. Moch, V. Pathak, N. Rana, and V. Ravindran, Phys. Rev. Lett. **133**, 211905 (2024), arXiv:2404.09959 [hep-ph].
- [14] S. Goyal, R. N. Lee, S.-O. Moch, V. Pathak, N. Rana, and V. Ravindran, Phys. Rev. D **111**, 094007 (2025), arXiv:2412.19309 [hep-ph].
- [15] M. Abele, D. de Florian, and W. Vogelsang, Phys. Rev. D **104**, 094046 (2021), arXiv:2109.00847 [hep-ph].
- [16] M. Abele, D. de Florian, and W. Vogelsang, Phys. Rev. D **106**, 014015 (2022), arXiv:2203.07928 [hep-ph].
- [17] V. Bertone, A. Chiefa, and E. R. Nocera (MAP), Phys. Lett. B **865**, 139497 (2025), arXiv:2404.04712 [hep-ph].
- [18] I. Borsa, M. Stratmann, W. Vogelsang, D. de Florian, and R. Sassot, Phys. Rev. Lett. **133**, 151901 (2024), arXiv:2407.11635 [hep-ph].
- [19] J. Cruz-Martinez, T. Hasenack, F. Hekhorn, G. Magni, E. R. Nocera, T. R. Rabemananjara, J. Rojo, T. Sharma, and G. van Seeventer, (2025), arXiv:2503.11814 [hep-ph].
- [20] V. Del Duca, L. J. Dixon, C. Duhr, and J. Pennington, JHEP **02**, 086, arXiv:1309.6647 [hep-ph].
- [21] L. J. Dixon, C. Duhr, and J. Pennington, JHEP **10**, 074, arXiv:1207.0186 [hep-th].
- [22] F. Chavez and C. Duhr, JHEP **11**, 114, arXiv:1209.2722 [hep-ph].

- [23] L. J. Dixon, E. Herrmann, K. Yan, and H. X. Zhu, JHEP **05**, 135, [Erratum: JHEP 06, 143 (2024)], arXiv:1912.09370 [hep-ph].
- [24] V. Del Duca and L. J. Dixon, J. Phys. A **55**, 443016 (2022), arXiv:2203.13026 [hep-th].
- [25] S. Abreu, G. De Laurentis, G. Falcioni, E. Gardi, C. Milloy, and L. Vernazza, JHEP **04**, 161, arXiv:2412.20578 [hep-ph].
- [26] K. Yan and X. Zhang, Phys. Rev. Lett. **129**, 021602 (2022), arXiv:2203.04349 [hep-th].
- [27] W. Furmanski and R. Petronzio, Z. Phys. C **11**, 293 (1982).
- [28] D. de Florian, M. Stratmann, and W. Vogelsang, Phys. Rev. D **57**, 5811 (1998), arXiv:hep-ph/9711387.
- [29] D. Anderle, D. de Florian, and Y. Rothe, Phys. Rev. D **95**, 034027 (2017), arXiv:1612.01293 [hep-ph].
- [30] T. Gehrmann and R. Schürmann, JHEP **04**, 031, arXiv:2201.06982 [hep-ph].
- [31] D. E. Knuth, Amer. Math. Monthly **99**, 403 (1992), arXiv:math/9205211 [math.HO].
- [32] K. Fabricius and I. Schmitt, Z. Phys. C **3**, 51 (1979).
- [33] T. Matsuura, S. C. van der Marck, and W. L. van Neerven, Nucl. Phys. B **319**, 570 (1989).
- [34] Z. Bern, L. J. Dixon, and D. A. Kosower, Nucl. Phys. B **412**, 751 (1994), arXiv:hep-ph/9306240.
- [35] E. B. Zijlstra and W. L. van Neerven, Nucl. Phys. B **383**, 525 (1992).
- [36] G. Duplancic and B. Nizic, Eur. Phys. J. C **20**, 357 (2001), arXiv:hep-ph/0006249.
- [37] V. E. Lyubovitskij, F. Wunder, and A. S. Zhevlakov, JHEP **06**, 066, arXiv:2102.08943 [hep-ph].
- [38] J. Haug and F. Wunder, JHEP **02**, 177, arXiv:2211.14110 [hep-ph].
- [39] J. Haug and F. Wunder, JHEP **05**, 059, arXiv:2302.01956 [hep-ph].
- [40] L. Lewin, *Structural properties of polylogarithms*, Mathematical Surveys and Monographs No. 37 (American Mathematical Soc., 1991).
- [41] E. E. Kummer, Journal für die reine und angewandte Mathematik **21**, 74 (1840).
- [42] L. J. Rogers, Proceedings of the London Mathematical Society **2**, 169 (1907).
- [43] D. Ramakrishnan, Contemp. Math **55**, 371 (1986).
- [44] Z. Wojtkowiak, Mathematica Scandinavica **65**, 140 (1989).
- [45] D. Zagier, in *Arithmetic Algebraic Geometry*, Progress in Mathematics No. 89, edited by G. van der Geer, F. Oort, J. Steenbrink (Springer, 1991) 1st ed., p. 391.
- [46] F. C. S. Brown, Compt. Rend. Math. **338**, 527 (2004).
- [47] S. J. Bloch, *Higher regulators, algebraic K-theory, and zeta functions of elliptic curves*, Vol. 11 (American Mathematical Soc., 2011).
- [48] O. Schnetz, Commun. Num. Theor. Phys. **08**, 589 (2014), arXiv:1302.6445 [math.NT].
- [49] F. Brown and O. Schnetz, J. Number Theor. **148**, 478 (2015).
- [50] J. Zhao, *Multiple zeta functions, multiple polylogarithms and their special values*, Vol. 12 (World Scientific, 2016).
- [51] J. Broedel, M. Sprenger, and A. Torres Orjuela, Nucl. Phys. B **915**, 394 (2017), arXiv:1606.08411 [hep-th].
- [52] C. Duhr and F. Dulat, JHEP **08** (2019), 135, arXiv:1904.07279 [hep-th].
- [53] S. Charlton, C. Duhr, and H. Gangl, SIGMA **17**, 107 (2021), arXiv:2104.04344 [math.NT].
- [54] H. Frost, M. Hidding, D. Kamlesh, C. Rodriguez, O. Schlotterer, and B. Verbeek, J. Phys. A **57**, 31LT01 (2024), arXiv:2312.00697 [hep-th].
- [55] O. Almelid, C. Duhr, and E. Gardi, Phys. Rev. Lett. **117**, 172002 (2016), arXiv:1507.00047 [hep-ph].
- [56] A. C. Petkou, Phys. Lett. B **820**, 136467 (2021), arXiv:2105.03530 [hep-th].
- [57] A. Voigt, (2022), arXiv:2201.01678 [hep-ph].
- [58] D. Binosi and L. Theußl, Comput. Phys. Commun. **161**, 76 (2004), arXiv:hep-ph/0309015.